LETTER

ACS chemical biology

Arginine Grafting to Endow Cell Permeability

Stephen M. Fuchs[†,‡] and Ronald T. Raines[†,§,*]

[†]Department of Biochemistry and [§]Department of Chemistry, University of Wisconsin–Madison, Madison, Wisconsin 53706, [‡]Present address: Lineberger Comprehensive Cancer Center, The University of North Carolina at Chapel Hill, Chapel Hill, North Carolina 27599

ABSTRACT We report on a means to endow proteins with the ability to permeate mammalian cells without appending an exogenous domain. Our approach is to install a cationic patch on the surface of a target protein by the grafting of arginine residues. Doing so with GFP did not compromise conformational stability but enabled efficient cellular uptake that was dependent on cell-surface glycosaminoglycans. We anticipate that this cell-permeable variant of GFP, which obviates the need for transfection, will be useful for numerous applications in cell biology and that the method of arginine grafting will be broadly applicable.

The plasma membrane is a natural barrier that excludes most molecules. Breaching this barrier is a limiting factor in the development of proteins and other biomolecules as therapeutics and diagnostic tools (*1*). Accordingly, there is much interest in developing new means to deliver proteins and other macromolecules into cells.

Small cationic peptides are capable of cellular entry, promoted best by the guanidinium group on the side chain of arginine residues (*2*–*4*). Appending polyarginine to proteins can enable uptake, but the transducing domain increases the size of a target protein and is readily susceptible to proteolysis (*5*). Chemical modification to supply a protein with cationic functional groups can likewise enable cellular entry (*6, 7*), but at the expense of homogeneity. Some ribonucleases are known to invade mammalian cells (*8*), perhaps as a result of a natural cluster of cationic residues on their surface (*9*). These precedents inspired us to use site-directed mutagenesis to modify a 3D scaffold with the intent of endowing cell permeability.

As a model, we chose to employ GFP from the jellyfish *Aequorea victoria*. GFP is a well-characterized protein (*10*–*13*) with a convenient signal, intrinsic fluorescence, for detecting cellular uptake (*14, 15*). More specifically, we made amino acid substitutions in enhanced GFP (eGFP), which is the F64L/S65T variant and has desirable fluorescence properties (*16*).

GFP is an acidic protein, having a net charge (*i.e.*, Arg + Lys − Asp − Glu) of $Z = -9$ at neutral pH. We noted that one face of GFP is variegated with acidic and basic residues (Figure 1). We chose to replace the five acidic residues (Glu17, Asp19, Asp21, Glu111, and Glu124) on this face with arginine. These acidic residues reside on three adjacent β-strands, proximal to five basic residues (Lys107, Arg109, Lys113, Lys122, and Lys126). Hence, these five substitutions created a highly cationic patch on the surface of eGFP (Figure 1), yielding a nearly neutral ($Z = +1$) variant that we refer to as cell-permeable GFP (cpGFP).

We produced cpGFP in *Escherichia coli* (*17*). Cation-exchange chromatography was especially efficacious in the purification of cpGFP, affording nearly homogeneous protein. The fluorescence properties of cpGFP were found to be nearly identical to those of eGFP (see Supporting Information).

Formation of the GFP fluorophore (*18, 19*) requires its proper folding (*20*). Moreover, use of GFP requires the retention of its conformational stability in biological assays. Replacing anionic residues with cationic ones can alter protein stability, though this effect is not readily predictable (*21*). Hence, we used chemical denaturation to ascertain the effect of arginine grafting on the stability of eGFP. We observed that both cpGFP and eGFP have unfolding midpoints at $C_{1/2} = 3.1 \pm 0.3$ M guanidine-HCl (see Supporting Information). Thus, the creation of a cationic patch did not have a deleterious effect on conformational stability.

Cellular internalization of GFP can be visualized by fluorescence microscopy (*14, 15*). Hence, we incubated HeLa cells with increasing concentrations of either cpGFP or

***Corresponding author,** raines@biochem.wisc.edu.

Received for review October 16, 2006 and accepted January 12, 2007.

Published online February 23, 2007

10.1021/cb600429k CCC: $37.00

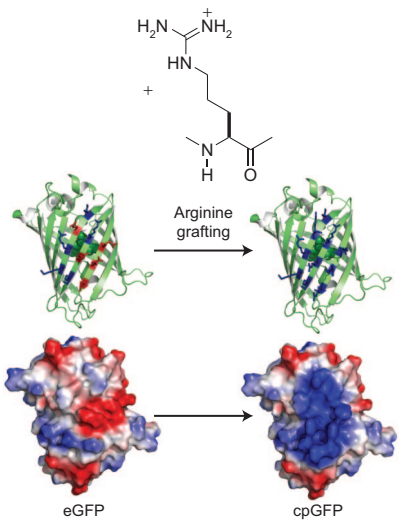

Figure 1. Scheme for arginine grafting to create a cpGFP. Top: ribbon model depicting the location of the five anionic residues in GFP that were replaced with arginine to yield a surface composed of 10 cationic residues. The fluorophore is depicted in space-filling mode. Bottom: space-filling model depicting the effect of the arginine substitutions on the electropotential surface (blue = cationic; red = anionic).

eGFP for known times at 37 °C. Prior to visualization, cells were placed in fresh medium for 1 h to allow for the internalization of any protein bound to the cell surface. We observed fluorescence within living cells incubated with cpGFP and found its intensity to be dose-dependent, increasing at high concentration of cpGFP (Figure 2, panels a–c). No cytotoxicity was observed, even upon incubation with 50 μM cpGFP. Although a small amount was detectable in the cytosol, cpGFP was observed primarily in vesicles. This localization is similar to that observed with cationic peptides such as polyarginine (*22*). Insignificant fluorescence intensity was observed in cells incubated with eGFP (Figure 2, panel d) or eGFP with a polyarginine appendage (*23*), though this latter experiment used neuronal cells and a much shorter incubation period.

Glycosaminoglycans (GAGs) such as heparan sulfate (HS) and condroitin sulfate (CS) on the cell surface can mediate the binding of cationic peptides and proteins (*4, 22, 24*). To probe for a role for GAGs in cpGFP internalization, we compared cell-surface binding and cellular internalization of cpGFP in wild-type Chinese hamster ovary (CHO) cells (CHO-KI) to that in a CHO cell line deficient in GAG biosynthesis. In wild-type CHO-K1 cells, cpGFP was observed to bind to the cell surface and undergo internalization (Figure 2, panel e). In CHO-745 cells (which are deficient in HS and CS), there is little internalization of cpGFP (Figure 2, panel f). At a 10-fold higher protein concentration, cpGFP is internalized in the GAG-deficient cell line (see Supporting Information). Similar results were obtained with another GAG-deficient cell line, CHO-677 (data not shown). Apparently, cpGFP internalization relies largely but not exclusively on the interaction with cell-surface GAGs and is efficient in both human and rodent cells displaying GAGs.

GFP and its variants are in widespread use in cell biology (*10, 12, 13*). Among these variants, cpGFP is unique in obviating a need for transfection or chemical additives to infuse mammalian cells with a fluorescent protein (*23*) and hence could have numerous applications, both *in vitro* and *in vivo* (*25*). For example, some GFP variants respond to changes in the solution pH or reduction potential (*17, 26*). Merging such variants with cpGFP could provide a useful sensor for important physicochemical parameters within living cells. Likewise, cpGFP could serve as a component of a FRET-based substrate for assays of proteolytic or other enzymatic activities (*27, 28*). More generally, our data demonstrate that an extraneous transduction domain (*2–4*) is not a necessary component of a cell-permeable protein. Accordingly, we anticipate that arginine grafting could become a useful means to endow many proteins with cell permeability.

METHODS

Materials. Plasmid pRSETB, which contains a complementary DNA (cDNA) for eGFP, was a gift from S. J. Remington (University of Oregon). Primers for making mutations in the eGFP cDNA were obtained from Integrated DNA Technologies (Coralville, IA) and had the sequences 5′-CACTGGAGTT GTCCCAATTCTTGTTCGTTTACGTGGTCGTGTTAATGGG

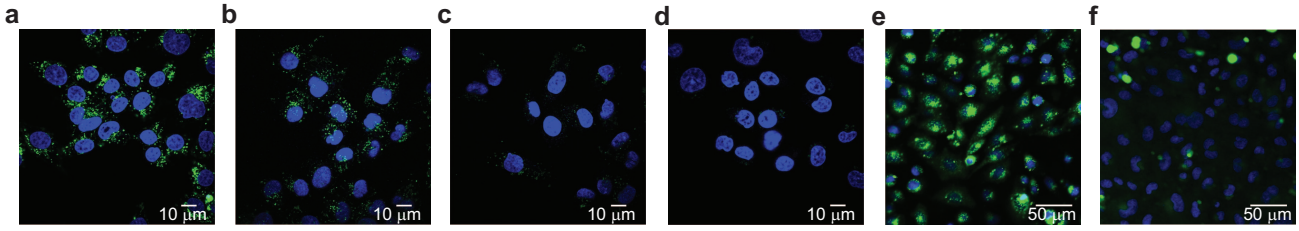

Figure 2. Images of the internalization of GFP variants into living human and rodent cells. HeLa cells were incubated with cpGFP (panel a, 10 μM; panel b, 1 μM; panel c, 0.1 μM) and eGFP (panel d, 10 μM) for 3 h in Opti-MEM medium at 37 °C. Cells were then placed in fresh medium for 1 h and stained with Hoechst 33342 (blue) and propidium iodide (red) for 15 min prior to visualization by confocal microscopy. GAG-deficient cells CHO-K1 (panel e) and CHO-745 (panel f) were incubated with cpGFP (2 μM) for 3 h at 37 °C in Opti-MEM medium. Cells were then placed in fresh medium for 1 h and stained with Hoechst 33342 (blue) and propidium iodide (red) for 15 min prior to visualization.

acs chemical biology

CACAAATTTTCTGTCAGTGG-3′ and its reverse complement (in which sites of mutation are underlined for the E17R, D19R, D21R substitutions), 5′-CGGGAACTACAAGACACGTGCTCGTGTCAAGTTTGAAGGTGATACCC-3′ and its reverse complement (for the E111R substitution), and 5′-CCCTTGTTAATAGAATCCGTTTAAAAGGTATTGATTTTAAAG-3′ and its reverse complement (for the E124R substitution). DH5α and BL21(DE3) competent cells were from Stratagene (La Jolla, CA).

Site-Directed Mutagenesis. cDNA encoding eGFP variants were produced by the QuikChange mutagenesis kit (Stratagene, La Jolla, CA) using the primer pairs described above. Three successive rounds of mutagenesis yielded cpGFP, which is an eGFP variant with five substitutions: E17R, D19R, D21R, E111R, and E124R.

Protein Production. Plasmids containing the sequences for eGFP and cpGFP were transformed into BL21(DE3) cells, and colonies were selected for on Luria–Bertani (LB) agar plates by their ampicillin (Amp) resistance. Small cultures (25 mL of LB medium containing 200 μg mL^{-1} Amp) were started from a single colony and grown at 37 °C with shaking at 200 rpm to an optical density of OD = 0.6 at 600 nm. One-liter cultures of the same medium were inoculated with 4 mL of the starter culture and grown at 37 °C with shaking at 300 rpm to OD = 0.6. Cultures were then cooled to 15 °C, and GFP cDNA expression was induced by the addition of isopropyl α-D-1-thiogalactopyranoside (final concentration: 1 mM). Cultures were grown at 15 °C with shaking at 300 rpm for 18 h and harvested by centrifugation (5000 rpm for 10 min) in a Beckman Coulter Avant J-20 XPI centrifuge using a JLA 8.1 rotor. Cell pellets were either frozen or used immediately in protein purification.

Protein Purification. Cell pellets from 1 L of cell culture were resuspended in ~10 mL of ice-cold cell lysis buffer (50 mM sodium phosphate buffer, pH 7.2, containing 500 mM NaCl and 1 mM phenylmethylsulfonyl fluoride). Cells were lysed by sonication (50% duty/50% output) 5 times for 30 s. Cell debris was removed by centrifugation at 22,000*g* for 60 min at 4 °C in a Beckman Optima XL-80K ultracentrifuge using a 60Ti rotor. Clarified cell lysate was dialyzed for at least 2 h against phosphate-buffered saline containing 500 mM NaCl (PBS+) (50 mM sodium phosphate buffer, pH 7.2, containing 636 mM NaCl) before loading onto a Ni–NTA agarose (Qiagen, Germany). The column was washed with the same buffer containing 20 mM imidazole before eluting with 50 mM sodium phosphate buffer, pH 7.2, containing NaCl (636 mM) and imidazole (500 mM). The fractions containing green-colored protein were pooled and diluted 1:10 with water to lower the salt concentration. cpGFP was then loaded onto a 5-mL HiTrap SP FF Sepharose column (Amersham Biosciences, Piscataway NJ). Protein was eluted with a 100-mL linear gradient (50 + 50 mL) of 50 mM sodium phosphate buffer, pH 7.5, containing NaCl (0–1.00 M). Fractions containing green-colored protein were pooled and dialyzed against 50 mM sodium phosphate buffer, pH 7.5, containing NaCl (652 mM). The N-terminal histidine tag was removed as described previously (*26*). Briefly, protein was incubated with 1:50 (w/w) α-chymotrypsin for 20 h at RT. Chymotrypsin degrades the N-terminal tag but does not cleave the GFP protein (*26*). Protein was concentrated using Vivascience 5000 MW spin columns and protein concentration was determined by optical absorbance at 280 nm (α_{280} = 19,890 $M^{-1}cm^{-1}$) or by the BioRad protein assay.

Fluorescence Spectroscopy. Fluorescence measurements were performed with a QuantaMaster 1 photon-counting spectrofluorimeter equipped with sample stirring (PhotonTechnology International, South Brunswick, NJ). Fluorescence excitation and emission spectra were obtained in PBS+ buffer using a 2-nm slit width and scanning at a rate of 1 nm s^{-1}.

Guanidine–HCl-Induced Equilibrium Unfolding. The conformational stability of GFP variants was determined by following the change in fluorescence as a function of denaturant concentration (*29*). GFP proteins (1–5 nM) were incubated in 96-well flat-bottom plates (total volume: 100 μL) in 50 mM sodium phosphate buffer, pH 7.5, containing NaCl (500 mM) and guanidine–HCl (0–6.30 M) for 24 h at RT. Fluorescence intensity was determined using a Tecan Ultra 384 fluorescence plate reader. Data were fitted to a two-state unfolding mechanism and could be used to calculate the standard free energy of denaturation: αG° ($= -RT\ln K$), where R is the gas constant, T is the absolute temperature, and K is the equilibrium constant calculated from the experimental data with the equation (*30, 31*): $K = [y\mathrm{N} - y]/[y - y\mathrm{D}]$. The value of y is the observed fluorescence value, and yN and yD are the y values for the native and denatured states, respectively.

Cell Internalization. HeLa cells, Chinese hamster ovary cells (CHO-K1), and GAG-deficient cell lines (CHO-677 and CHO-745) were obtained from the ATCC and maintained according to recommended instructions. The day before protein incubation, cells were seeded onto 4- or 8-well Lab-Tek II Chambered Coverglass tissue culture dishes (Nalge Nunc International, Naperville, IL) to yield 75% confluency on the next day. The following day, protein solutions (in PBS containing 500 mM NaCl) were added to cells in 200 μL (protein volume added was <1/20 of the total volume) of medium or PBS containing $MgCl_2$ (1 mM) and $CaCl_2$ (1 mM). Protein was incubated with cells for known times, and the cells were then washed with PBS containing magnesium and calcium three times prior to visualization. In some samples, cell nuclei were counterstained with Hoechst 33342 for 5 min prior to washing. Internalization was visualized with a Nikon C1 laser scanning confocal microscope equipped with 20x, 60x, and 100x lenses. Images were acquired as 512 x 512 pixel images representing a 636.5 μM (20x) or 27.3 μM (100x) window. All images were taken on the same day using the same laser intensity (~10% output). Images were taken as 3 x 3 in sections from the original file and reduced by 50% for publication.

Electrostatic Potential Diagrams. Electrostatic potential diagrams were made by using the atomic coordinates for F64L/S65T/Y66L GFP (Protein Data Bank entry 1S6Z (*32*)) and the program MacPyMol (DeLano Scientific, South San Francisco, CA). Default settings were used except that the Coulomb dielectric was set to be 80. A model of cpGFP was created and likewise modeled by using the program MacPyMOL.

Acknowledgments: The authors would like to thank G. T. Hanson for contributive discussions and F. W. Kotch and M. Paul for advice on the manuscript. S.M.F. was supported by Biotechnology Training Grant 08349 National Institutes of Health (NIH). This work was supported by grants GM44783 and CA73808 (NIH).

Supporting Information Available: This material is available free of charge *via* the Internet.

REFERENCES

1. Marafino, B. J., Jr., and Pugsley, M. K. (2003) Commercial development considerations for biotechnology-derived therapeutics, *Cardiovasc. Toxicol. 3*, 5–12.
2. Yang, Y., Ma, J., Song, Z., and Wu, M. (2002) HIV-1 TAT-mediated protein transduction and subcellular localization using novel expression vectors, *FEBS Lett. 532*, 36–44.
3. Fischer, R., Fotin-Mleczek, M., Hufnagel, H., and Brock, R. (2005) Break on through to the other side–biophysics and cell biology shed light on cell-penetrating peptides, *ChemBioChem 6*, 2126–2142.
4. Fuchs, S. M., and Raines, R. T. (2006) Internalization of cationic peptides: the road less (or more) traveled, *Cell. Mol. Life Sci. 76*, 1819–1822.
5. Fuchs, S. M., and Raines, R. T. (2005) Polyarginine as a multifunctional fusion tag, *Protein Sci. 14*, 1538–1544.
6. Triguero, D., Buciak, J. B., Yang, J., and Pardridge, W. M. (1989) Blood-brain barrier transport of cationized immunoglobulin G: enhanced delivery compared to native protein, *Proc. Natl. Acad. Sci. U.S.A. 86*, 4761–4765.
7. Futami, J., Kitazoe, M., Maeda, T., Nukui, E., Sakaguchi, M., Kosaka, J., Miyazaki, M., Kosaka, M., Tada, H., Seno, M., Sasaki, J., Huh, N. H., Namba, M., and Yamada, H. (2005) Intracellular delivery of proteins into mammalian living cells by polyethylenimine-cationization, *J. Biosci. Bioeng. 99*, 95–103.
8. Haigis, M. C., and Raines, R. T. (2003) Secretory ribonucleases are internalized by a dynamin-independent endocytic pathway, *J. Cell Sci. 116*, 313–324.
9. Notomista, E., Mancheño, J. M., Crescenzi, O., Di Donato, A., Gavilanes, J., and D'Alessio, G. (2006) The role of electrostatic interactions in the antitumor activity of dimeric RNases, *FEBS J. 273*, 3687–3697.
10. Zimmer, M. (2005) *Glowing Genes: A Revolution in Biotechnology*, Prometheus Books, Amherst, NY.
11. Pieribone, V., and Gruber, D.F. (2006) *Aglow in the Dark: The Revolutionary Science of Biofluorescence*, Belknap Press, Cambridge, MA.
12. Ward, T. H., and Lippincott-Schwartz, J. (2006) The uses of green fluorescent protein in mammalian cells, *Methods Biochem. Anal. 47*, 305–337.

13. Zacharias, D. A., and Tsien, R. Y. (2006) Molecular biology and mutation of green fluorescent protein, *Methods Biochem. Anal. 47*, 83–120.
14. Han, K., Jeon, M.-J., Kim, K.-A., Park, J., and Choi, S. Y. (2000) Efficient intracellular delivery of GFP by homeodomains of *Drosophila* Fushi-tarazu and engrailed proteins, *Mol. Cells 10*, 728–732.
15. Tanaka, Y., Dowdy, S. F., Linehan, D. C., Eberlein, T. J., and Goedegebuure, P. S. (2001) Induction of antigen-specific CTL by recombinant HIV transactivating fusion protein-pulsed human monocyte-derived dendritic cells, *J. Immunol. 170*, 1291–1298.
16. Cormack, B. P., Valdivia, R. H., and Falkow, S. (1996) FACS-Optimized mutants of the green fluorescent protein (GFP), *Gene 173*, 33–38.
17. Hanson, G. T., McAnaney, T. B., Park, E. S., Rendell, M. E., Yarbrough, D. K., Chu, S., Xi, L., Boxer, S. G., Montrose, M. H., and Remington, S. J. (2002) Green fluorescent protein variants as ratiometric dual emission pH sensors. 1. Structural characterization and preliminary application, *Biochemistry 41*, 15477–15488.
18. Cody, C. W., Prasher, D. C., Westler, W. M., Prendergast, F. G., and Ward, W. W. (1993) Chemical structure of the hexapeptide chromophore of the *Aequorea* green-fluorescent protein, *Biochemistry 32*, 1212–1218.
19. Bell, A. F., He, X., Wachter, R. M., and Tonge, P. J. (2000) Probing the ground state structure of the green fluorescent protein chromophore using Raman spectroscopy, *Biochemistry 39*, 4423–4431.
20. Waldo, G. S., Standish, B. M., Berendzen, J., and Terwilliger, T. C. (1999) Rapid protein-folding assay using green fluorescent protein, *Nat. Biotechnol. 17*, 691–695.
21. Pace, C. N., Alston, R. W., and Shaw, K. L. (2000) Charge–charge interactions influence the denatured state ensemble and contribute to protein stability, *Protein Sci. 9*, 1395–1398.
22. Fuchs, S. M., and Raines, R. T. (2004) Pathway for polyarginine entry into mammalian cells, *Biochemistry 43*, 2438–2444.
23. Takeuchi, T., Kosuge, M., Tadokoro, A., Sugiura, Y., Nishi, M., Kawata, M., Sakai, N., Matile, S., and Futaki, S. (2006) Direct and rapid cytosolic delivery using cell-penetrating peptides mediated by pyrenebutyrate, *ACS Chem. Biol. 1*, 299–303.
24. Richard, J. P., Melikov, K., Brooks, H., Prevot, P., Lebleu, B., and Chernomordik, L. V. (2005) Cellular uptake of unconjugated TAT peptide involves clathrin-dependent endocytosis and heparan sulfate receptors, *J. Biol. Chem. 280*, 15300–15306.
25. Hoffman, R. M. (2005) The multiple uses of fluorescent proteins to visualize cancer in vivo, *Nat. Rev. Cancer 5*, 796–806.
26. Hanson, G. T., Aggeler, R., Oglesbee, D., Cannon, M., Capaldi, R. A., Tsien, R. Y., and Remington, S. J. (2004) Investigating mitochondrial redox potential with redox-sensitive green fluorescent protein indicators, *J. Biol. Chem. 279*, 13044–13053.
27. Heim, R., and Tsien, R. Y. (1996) Engineering green fluorescent protein for improved brightness, longer wavelengths and fluorescence resonance energy transfer, *Curr. Biol. 6*, 178–182.
28. Pollok, B. A., and Heim, R. (1999) Using GFP in FRET-based applications, *Trends Cell Biol. 9*, 57–60.
29. Stepanenko, O. V., Verkhusha, V. V., Kazakov, V. I., Shavlovsky, M. M., Kuznetsova, I.M., Uversky, V. N., and Turoverov, K. K. (2004) Comparative studies on the structure and stability of fluorescent proteins EGFP, zFP506, mRFP1, "dimer2", and DsRed1, *Biochemistry 43*, 14913–14923.
30. Tanford, C. (1968) Protein denaturation, *Adv. Protein Chem. 23*, 121–282.
31. Pace, C. N., and Scholtz, J.M. (1997) Measuring the conformational stability of a protein, in *Protein Structure* (Creighton, T. E., Ed.) pp 299–321, Oxford University Press, New York.
32. Rosenow, M. A., Huffman, H. A., Phail, M. E., and Wachter, R. M. (2004) The crystal structure of the Y66L variant of green fluorescent protein supports a cyclization–oxidation–dehydration mechanism for chromophore maturation, *Biochemistry 43*, 4464–4472.